

## SPEED OF SOUND IN PURE WATER AT TEMPERATURE BETWEEN 274 AND 394 K AND PRESSURE UP TO 90 MPa BY ULTRASONIC PULSE-ECHO TECHNIQUE

G. Benedetto, R. M. Gavioso, P. A. Giuliano Albo, S. Lago, D. Madonna Ripa and R. Spagnolo

<sup>1</sup> Istituto Elettrotecnico Nazionale «Galileo Ferraris», Torino, ITALIA

lago@ien.it

### Abstract

A newly designed experimental apparatus suitable for speed of sound measurements in high-pressure liquids up to 90 MPa has been used to determine the speed of sound in high purity water on the temperature range from 274 K and 394 K with an estimated accuracy of 0.05%. Experimental speed of sound data were combined with published density and heat capacity data on one isobar at low pressure, to obtain values for the same quantities and other related thermodynamic properties over the whole temperature and pressure range, by means of numerical integration technique. Obtained results were compared with data from available reference sources.

### Introduction

Besides its basic importance in a great number of different technical and scientific applications, water is commonly used as a reference fluid for the calibration of a variety of measuring devices, including experimental apparatus for the measurement of the speed of sound in liquids. As a part of an ongoing research program to develop an accurate experimental technique for the speed of sound measurements in high pressure liquids, we considered the possibility to avoid such a calibration procedure, and obtain at the same time values of speed of sound in pure water of profitable accuracy.

The speed of sound in water as a function of temperature and pressures has been extensively measured by the application of a variety of methods, nevertheless results of very high accuracy are typically available only at atmospheric pressure [1][2], or over a limited range of temperature at higher pressures [3][4][5].

In this work we report measurements of speed of sound  $u$  in pure water at temperatures between 274 and 394 K and pressures up to 90 MPa. These results have been compared to those calculated from the International Association for the Properties of Water and Steam (IAPWS-95) formulation [6] and are in agreement within 0.1% over the whole investigated temperature and pressure range.

Accurate measurements of the speed of sound in real fluids have a special interest as they offer an indirect way to obtain information on related thermodynamic properties like density and heat capacity, whose direct measurement, especially at high pressure, is extremely difficult. In order to test this possibility, we combined our acoustic data with values of density  $\rho$  and isobaric

specific heat capacity  $c_p$  calculated from IAPWS-95 formulation [6] on an arbitrary isobar at 0.1 MPa and, by means of the integration technique described below, determined the same quantities over the entire  $P$ - $T$  region investigated by this study.

### Experimental Apparatus

The design of the present ultrasonic apparatus is based on the double reflector pulse-echo technique [7][8] and it has been chosen in reason of its good combination of design simplicity and high achievable resolution and accuracy.

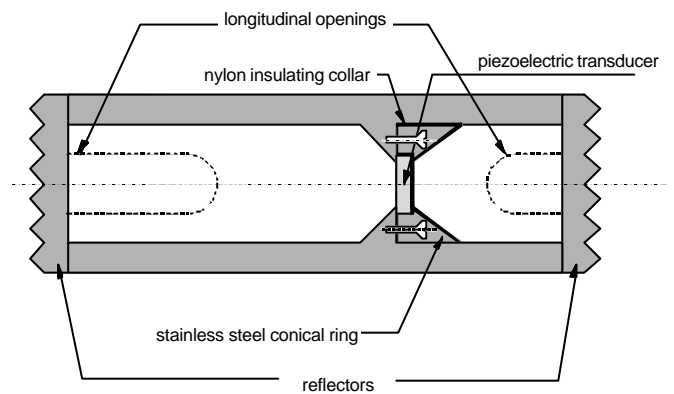


Figure 1: Ultrasonic cell

A diagram of the ultrasonic cell is shown in fig.1. It is made of a hollow AISI 303 stainless steel cylinder (77 mm long, o.d. 43 mm, i.d. 33 mm) in which the ultrasonic transducer, a piezoelectric (PbZrTiO<sub>3</sub> – Channel Industries mod. C5400) disk (diam. 10 mm, thickness 0.5 mm), is clamped at its edges between a conical support and a conical teflon insulated stainless steel ring. The conical shape of the ring and the support minimizes the interfering effect of diverging components of the acoustic beam which may be reflected on the transducer. The ring and the support are fixed to each other by means of three screws electrically insulated by small teflon collars. Two solid stainless steel reflectors (thickness 15 mm), having plane smooth surfaces, are fixed to the bases of the cell respectively at a distance of 30.5 and 46 mm. The outer surfaces of the reflectors were cut with a series of pyramid-shaped incisions in order to maximize dispersion of sound passing through the reflectors, thus avoiding its back-reflection into the cell.

### Measurement of propagation time

Ultrasonic measurement of speed of sound basically consists in the determination of two mechanical quantities: a geometric acoustic path and the associated time delay. According to the double reflector pulse-echo ultrasonic technique, a function generator (Agilent 33250A) excites the piezo-ceramic transducer with an electrical signal in the form of ten-cycle repeated tone bursts with a carrier frequency of about 5 MHz and an amplitude of  $10 V_{p-p}$ . The transducer emits simultaneously two acoustic pulses in opposite directions. Each acoustic wave train, hitting the reflector, produces a set of echoes. The electrical signal delivered to the transducer and the echoes from the reflectors are recorded by a digital oscilloscope (LeCroy LT372). The complete waveform corresponds to a duration of 100  $\mu s$  and it is digitized at a sampling rate of  $4 \cdot 10^9$  samples per second. The digital signal  $P_1(t_i)$ , representing the first sampled echo coming from the nearest reflector, is correlated to the first echo  $P_2(t_j)$  from the furthest reflector by means of a temporal correlation function

$$C(\mathbf{t}) = \int_{-\infty}^{+\infty} P_1(t)P_2(t + \mathbf{t})dt \quad (1)$$

where  $\mathbf{t} \in ]-\infty, +\infty[$  is a point in the delay-time domain. A fast and reliable method to accomplish this calculation is based on the FFT algorithm and the properties of Fourier transforms: applying the Fourier operator  $F[...]$  to both sides of (1), we obtained

$$F[C] = F[P_1]^* F[P_2]. \quad (2)$$

The correlation function is obtained at the cost of two FFT transforms and a final inverse transform on  $F[C]$ . The delay time between the two echo waveforms  $P_1(t_i)$  and  $P_2(t_j)$  is assumed as the value  $t_{exp}$  which maximizes the function  $C(\mathbf{t})$ . This method has the main advantage of being insensitive to amplitude differences between the two echo waveforms. The performance of the algorithm has been tested with synthetic data and found to be very robust: the addition of gaussian noise, with an amplitude equal to 10% of the maximum signal, produced a difference of only one sampling interval in the determination of the delay time.

### Dimensional Measurements

A coordinate measuring machine was used to determine the difference  $DL$  between the length of the acoustic paths  $L_1$  (length existing between the transducer and the nearest reflector) and  $L_2$  (length existing between the transducer and the furthest reflector). The machine had a resolution and a repeatability of 0.1  $\mu m$  and an accuracy of

approximately 1  $\mu m$ . Measurements were carried out in a thermostatted room at ambient pressure  $P_0$ . Five successive measuring sequences were accomplished, each one consisting of nine randomly spaced points on the two surfaces of the PZT transducer and on the flat faces of the cell sidewall. The maximum difference between the five evaluations of  $L_{1,2}$  was less than 1  $\mu m$ . Though it is likely that the major unknown systematic uncertainty components associated to the coordinates measurement would cancel out in the difference operation, we associated the uncertainty of  $\pm 2 \mu m$  to the determined values  $L_1 = 30.592$  mm and  $L_2 = 45.997$  mm. Finally the determined difference in the acoustic path was  $DL = (15.405 \pm 0.004)$  mm. The variation of  $DL$  with temperature and pressure was calculated as  $DL(T, P) = DL(T_0, P_0)(1 + aDT + bDP)$ , where  $a$  and  $b$  are respectively the coefficients of thermal expansion [10] and the coefficient of compressibility of 303 stainless steel; the latest was calculated from the values of the elastic constants of the same material. The magnitude of the corrections, required for the path length, were 0.034% at the maximum pressure (90 MPa) and temperature (394 K).

### High pressure system

The high pressure system consists of three main sections: the pressure vessel, a pressure monitoring and measuring line and a pressure control device. Pressure is generated and controlled by a 100 MPa pressure amplifier connected to an ambient pressure liquid reservoir which contains the sample under test. A pressure transducer (Sensotec TJE/4843-01) was used to measure the pressure in the system with an uncertainty of 0.04 MPa as estimated from the calibration between 20 and 90 MPa by a pressure balance (national standard). The pressure vessel, specifically designed for this application, is made from a stainless steel alloy and has an internal volume of 420  $cm^3$ . It is provided with two coaxial pressure-tight electrical feedthroughs for high frequency signals transmission to the ultrasonic cell and can be operated with pressures up to 100 MPa and in a temperature range of (230÷400) K.

### Temperature measurement and control

The ultrasonic cell and the pressure vessel were placed in a stirred liquid bath thermostat, based on a dewar vessel with a capacity of approximately 60  $dm^3$ . The fluid within the bath was a silicone oil (Dow Corning 200/100cs). Temperature was maintained and controlled by a system consisting of a main thermostat (Julabo FP50), having a stability of  $\pm 0.01$  K, and a proportional integral derivative (PID) controller, operating with a platinum resistance probe and a 60 W incandescence bulb which served as the control

heater. This system permitted to achieve a long-term temperature stability within the bath of  $\pm 2$  mK over the whole operating temperature range. The temperature associated to speed of sound measurements was determined with an accuracy of  $\pm 0.01$  K as the average of the readings of two platinum resistance thermometers (PRTs) (calibrated by comparison with a standard PRT), which were placed to the top and bottom parts of the pressure vessel. The temperature gradient recorded, by the two PRTs in the course of the present speed of sound measurements, was within 10 mK, with the exception of the lowest isotherm at 274 K; in this case the top of the vessel was 20 mK warmer than the bottom suggesting that a thermal link from the top to ambient temperature existed.

### Speed of sound in water. Results and comparison with IAPWS-95

Measurements were carried out on nine isotherms between 274 K and 394 K, in approximately 10 MPa pressure decrements from 90 MPa to atmospheric pressure, with the exception of the two last isotherms (379 K and 394 K), where were limited to the minimum pressure of 10 MPa, due to the sample being in the vapour state at atmospheric pressure.

We have compared our results to the predictions of the IAPWS-95 formulation. The estimated uncertainty of the formulation in speed of sound ranges from  $\pm 0.005\%$  at atmospheric pressure to a maximum of  $\pm 0.1\%$  over the  $P$ - $T$  region interested by the measurements.

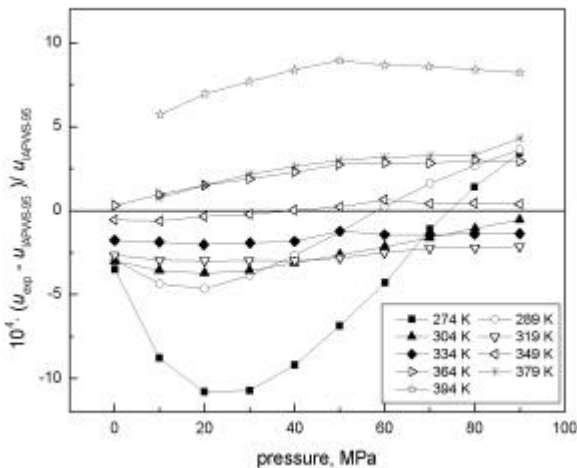


Figure 2: Deviations of experimental speed of sound in water from IAPWS-95 formulation

As represented in fig. 2, most of obtained results show deviations from IAPWS-95 within 0.05%, with the exception of the lowest and highest temperature

isotherms at 274 K and 394 K, whose deviations are within 0.1%.

The smoothness and low scatter of the deviations show the satisfactory level of precision achieved with the present experimental apparatus and measurement procedures.

### Derivation of density and isobaric heat capacity

From the experimental sound speed data points, it is possible to work out the density function  $\mathbf{r}(T, P)$ , i.e. the equation of state of the fluid under test, and the isobaric specific heat capacity function  $c_p(T, P)$  over the  $P$ - $T$  region examined, given a set of independent  $\mathbf{r}$  and  $c_p$  determinations on a single (but otherwise arbitrary) isobar.

The starting relations are

$$\left(\frac{\partial \mathbf{r}}{\partial P}\right)_T = \frac{T \mathbf{a}_p^2}{c_p} + \frac{1}{u^2} \quad (3)$$

$$\left(\frac{\partial c_p}{\partial P}\right)_T = -\frac{T}{\mathbf{r}} \left[ \mathbf{a}_p^2 + \left(\frac{\partial \mathbf{a}_p}{\partial T}\right)_P \right] \quad (4)$$

$$\mathbf{a}_p = -\frac{1}{\mathbf{r}} \left(\frac{\partial \mathbf{r}}{\partial T}\right)_P, \quad (5)$$

where  $\mathbf{a}_p$  is the thermal expansion coefficient and  $u$  the sound speed. Given a suitable initial condition in the form of  $\mathbf{r}(T, P_0)$  and  $c_p(T, P_0)$  functions at the starting pressure  $P_0$ , equations (3-5) form a complete first order differential equations system that can be integrated over the entire pressure range covered by the  $u(T, P)$  function.

We used a Cash-Karp, adaptive step size Runge-Kutta method which provides a fifth order approximation to differential equations systems. Sound speed experimental data have been interpolated by means of the Akima algorithm [9], a locally bivariate quintic polynomial generator, in order to produce an orthogonal mesh of sound speed values in the  $P$ - $T$  space. The system of eqs. (3-5) was then integrated over the entire pressure and temperature range, using a B-SPLINE sixth order interpolating function to calculate the derivatives which appear in the equations. The integration program proceeded along nine isothermal lines starting from atmospheric pressure, apart from the last two isotherms (379 K and 394 K), which started from 10 MPa.

The integration procedure was first tested on speed of sound data drawn from [6] and found to reproduce density values from the same source obtaining a maximum relative deviation of 1 ppm. The corresponding agreement for isobaric heat capacities was within  $2 \cdot 10^{-4}$  with the only exception of the lower isotherm at 274 K, whose maximum deviation from

reference values was  $2 \cdot 10^{-3}$ . We consider this problem to be the result of an inaccurate evaluation of derivatives that appear in the right side of eq. (4) for points on the boundary of the integration region, as pointed out in [5].

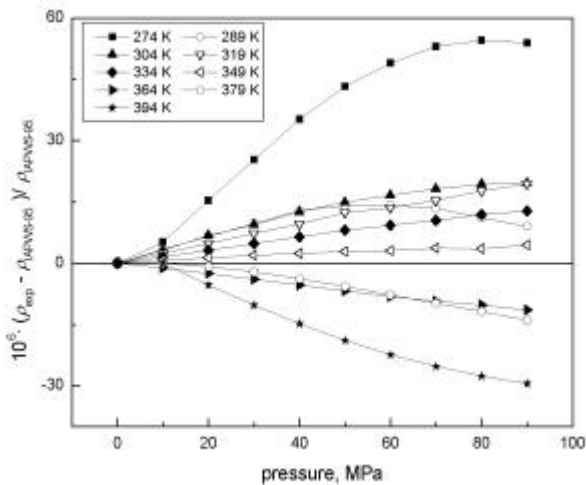


Figure 3: Deviation of calculated densities of water from IAPWS-95 formulation

A comparison between density data, calculated with the procedure discussed above from our experimental values of sound speed, and the reference values from IAPWS-95 is shown in fig. 3. It can be noted an overall good agreement, apart from the above mentioned anomaly at 274 K (the declared relative uncertainty for IAPWS-95 density data is  $\pm 10^{-5}$ ).

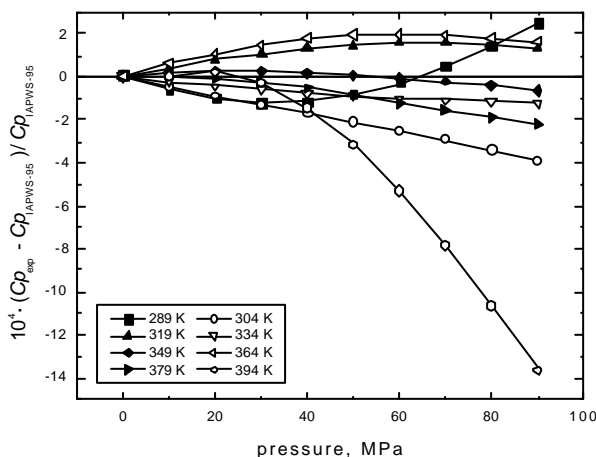


Figure 4: Deviation of calculated isobaric heat capacities of water from IAPWS-95 formulation

In fig. 4, the results of an analogous comparison for the calculated isobaric heat capacities is shown. The anomalous 274 K isotherm has been eliminated to

enhance graphical rendering. Apparently the greater deviations for the isotherm at 394 K are determined by the corresponding greater sound speed deviations from reference values which directly influence the algorithmic reconstruction of the  $c_p(T, P)$  function.

### Conclusions

Speed of sound measurements on samples of purified water in an extended region of  $P$ - $T$  space have been used to test a new assembled ultrasonic apparatus against available literature data. The results and the uncertainty evaluation demonstrate a good performance of the whole measurement system and suggest further improvements: a better precision and accuracy in the thermodynamic point determination and an improved piezo-clamping mechanism to guarantee a higher degree of parallelism between the ultrasonic source and the reflectors, reducing the uncertainty in the evaluation of the acoustic paths.

### References

Transaction, Proceedings or Journal Articles:

- [1] V. A. Del Grosso, C.W. Mader, *J. Acoust. Soc. Am.* **52**: 1441(1972)
- [2] K. Fujii, R. Masui, *J. Acoust. Soc. Am.* **93**: 276(1993)
- [3] K. Fujii, paper presented at the 13<sup>th</sup> Symposium on Thermophysical Properties, Boulder, Colorado, USA (1997)
- [4] A.A. Alexandov, A.I. Kochetov, *Therm. Eng.* **26**: 558(1979).
- [5] J.P. Petitet, R. Tufeu, B. La Neindre, *Int. J. Thermophys.* **4**: 35(1983)
- [6] W. Wagner, A. Pruss, *J. Phys. Chem. Ref. Data* **31**: 387(2002)
- [7] P.J. Kortbeek, M.J.P. Muringer, N.J. Trappeniers, S.N. Biswas, *Rev. Sci. Instrum.* **56**: 1269, (1985).
- [8] S. J. Ball, J.P.M. Trusler, *Int. J. Thermophys.* **22**: 427(2001).
- [9] H. Akima, *ACM Trans. Math. Softw.* **4**: 148 (1978).

Book :

- [10] ASM Committee on wrought stainless steels, in *Metals Handbook* (9<sup>th</sup> ed., American Society for Metals, 1980).